Journal of Mechanical Science and Technology 33 (2) (2019) 711~719
www.springerlink.com/content/1738-494x(Print)/1976-3824(Online)
DOI 10.1007/s12206-019-0125-4

Application of a layerwise theory for efficient topology optimization of laminate structure †

Jong Wook Lee[1], Jong Jin Kim[1], Heung Soo Kim[2] and Gil Ho Yoon[3,*]

[1]*Graduate School of Mechanical Engineering, Hanyang University, Seoul, Korea*
[2]*Department of Mechanical, Robotics and Energy Engineering, Dongguk University, Seoul, Korea*
[3]*School of Mechanical Engineering, Hanyang University, Seoul, Korea*

(Manuscript Received January 23, 2018; Revised August 24, 2018; Accepted October 25, 2018)

Abstract

This research applies a layerwise theory to topologically optimize laminate composite. As laminate composite structures are consisted of many thin layers, some limitations exist in analyzing and optimizing based on linear plate or shell theory. To overcome these limitations and problems, various layerwise theories have been developed. Thus, more accurate solutions can be efficiently obtained by these layerwise theories. In this research, one of the layerwise theory is applied to topologically optimize laminate structures. In the forward analysis for structural displacements, it is possible to efficiently conduct a numerical analysis and the sensitivity analysis in topology optimization. By solving several numerical examples, we observed that the directions of optimal layouts are different from each other depending on the type of load applied. Also, various design shapes were drawn to complement the difference in stiffness due to the rotation of each layer. In addition, an analysis of how the various combinations of angles and their position affect the stiffness was also discussed in this study.

Keywords: Compliance minimization; Composite material; Laminate structure; Layerwies theory; Topology optimization

1. Introduction

Composites are widely used throughout industry field due to their ability having better mechanical performance than they were in the original state. Many researches about composite have been reported and composites have verified their performances by experiment or computational simulations. Composites are generally made by stacking of thin composite plates (see Fig. 1). Each layer also can have different mechanical properties or strengths. In addition, even with a same anisotropic material, different mechanical properties can be utilized depending on the rotation angle of each layer. To predict the mechanical behaviors of composite, a classical plate theory was firstly used to compute the displacement of the laminated composite structure [1-3].

The conventional plate and shell theories cannot accurately predict the behaviors of thick laminated composite structures because the transverse shear deformation is simplified in these theories [1, 3]. In the case of thinner composite structure, the simplifying or neglecting the effect of the shear deformation can be possible. In case of thicker composite structure, the

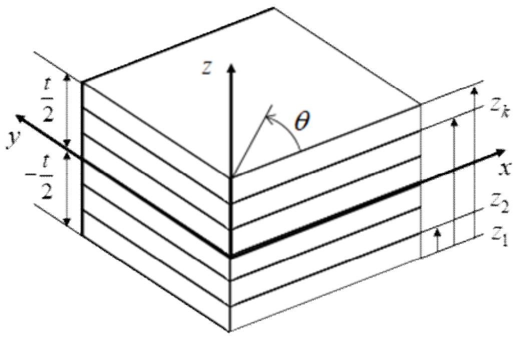

Fig. 1. General configuration of laminate composite structure.

simplifying or neglecting of the effect of the shear deformation causes large errors in predicting mechanical behavior. For instance, the shear correction factor is used in the first order shear deformation theory and the tangential transverse shear effect is used in the high order theory [3]. Although these methods are applicable in the mechanical problem with a single layer problem, some other issues have to be solved for the application to laminated composite structure composed of several layers. Therefore, the zigzag shape function of in-plane displacements and the inter laminar continuity of transverse stresses were developed [4-7]. Recently a theory called

*Corresponding author. Tel.: +82 2 2220 0451, Fax.: +82 2 2220 2299
E-mail address: ghy@hanyang.ac.kr, gilho.yoon@gmail.com
† Recommended by Associate Editor Kyeongsik Woo

the layerwise theory was introduced solving the zig-zag displacement issue and the inter-laminar continuity of transverse stresses issue [8-12]. Unfortunately, these theories still possess an issue of many dominant variables depending on the number of layers. Recently, an improved layerwise theory accurately estimating stresses or strains and saving the computational cost was presented [3, 13-18]. As this improved layerwise theory employs the zig-zag shape function with small number of unknown variables, computation time is slightly decreased by applying continuity conditions. Furthermore, it can accurately predict the zigzag shape of in-plane displacement and the transverse shear stress continuity is satisfied at all inter laminar surfaces. For more information, see Refs. [3, 16-18] and references therein.

This research presents the topology optimization of laminar composite structure based on the layerwise theory. Topology optimization was introduced in the late 1980s and many researches and applications have been reported (see Refs. [19-30] and references therein). To our knowledge, there are few researches in topology optimization for laminate composite structure. In Refs. [31-35], the classical plate theory was applied in structural optimization. These researches are applicable to thin laminate composite structures and the accurate calculations of displacements, strains and stresses are not limited [31-35]. Recently, interest in energy harvesting technology has been increasing, and studies have been carried out to apply topology optimization method to piezoelectricity material to maximize power generation or electromechanical coupling coefficient [36-39]. And even then, classical plate theory has been used for analysis. The layerwise theory employed in the present topology optimization study can accurately compute displacements and stresses regardless of the number of composite layers and the thickness of the structure. Furthermore, computational cost can be extremely saved because the primary variables independent of the number of layers are used in this theory.

To show the validity and the efficiency of the present development, the compliance minimization problems of laminated composite structure are solved; the compliance minimization problem subject to the mass constraint. In addition to the design variables defining void domain or solid domain, i.e., densities of each finite element, the angles of each layers are optimized simultaneously. By optimizing these angles, some significant improvements in compliance can be achievable.

The present research is organized as follows: In Sec. 2, the layerwise theory is described in short. And the computational efficiency is shown by comparing the computation times spent by 3-dimensional FE analysis and the layerwise theory. Sec. 2 also presents the topology optimization theory and the sensitivity analysis of the layerwise theory. Sec. 3 solves several optimization problems to show the efficiency of the present developments. In Sec. 4, some discussions are presented.

2. Composite laminate structure formulation and topology optimization

2.1 Mathematical theory – improved layerwise theory

Composite laminate structures being consisted of thin or thick layers, 3-dimensional FE analysis requires a lot of computational resources for accurate response computation for displacements and stresses. To overcome these limitations, some classical plate theories were developed by simplifying or neglecting the influence of transverse shear deformation. As discussed in the introduction, the layerwise theory was developed for the purpose of overcoming this limitation of some classical plate theories [3, 13-18]. Improved predictions of displacements and stresses are possible with the help of the layerwise theory. Displacement fields in the layerwise theory are approximated as follows [16-18]:

$$\begin{aligned} U_x^k(x,y,z) &= u_x(x,y) + \phi_x(x,y)z + \theta_x^k(x,y)g(z) + \psi_x^k(x,y)h(z) \\ U_y^k(x,y,z) &= u_y(x,y) + \phi_y(x,y)z + \theta_y^k(x,y)g(z) + \psi_y^k(x,y)h(z) \\ U_z^k(x,y,z) &= w(x,y) \end{aligned} \tag{1}$$

where U_x^k and U_y^k denote the in-plane displacements of the k-th layer of the laminate and U_z^k denotes the transverse deflection of the k-th layer or ply of the laminate. The quantities u_x, u_y and w denote the displacements of the reference plane. The rotations of the normal to the reference plane about x and y axes are ϕ_x and ϕ_y. The terms θ_x^k, θ_y^k, ψ_x^k and ψ_y^k are the layerwise structural unknowns defined at the k-th ply. The through-laminate-thickness functions, $g(z)$ and $h(z)$, are used to address the characteristics of in-plane zigzag deformations and have the following forms.

$$\begin{aligned} g(z) &= \sinh(z/t) \\ h(z) &= \cosh(z/t) \end{aligned} \tag{2}$$

where t is the total thickness of laminate structure and the functions $g(z)$ and $h(z)$ render high order odd and even distributions, respectively.

The assumed layerwise displacement field can be further simplified by applying the structural constraints [16-18] in order to reduce the number of structural variables. Here, applied structural conditions are traction free boundary conditions on top and bottom and continuity conditions of transverse shear stress and in-plane displacement on each inter-laminar. By applying these conditions, modified in-plane displacement fields are presented as follows:

$$\begin{aligned} U_x^k(x,y,z) &= u_x + A_x^k(z)\phi_x + B_x^k(z)\phi_y + C_x^k(z)w_{,x} + D_x^k(z)w_{,y} \\ U_y^k(x,y,z) &= u_y + A_y^k(z)\phi_x + B_y^k(z)\phi_y + C_y^k(z)w_{,x} + D_y^k(z)w_{,y} \end{aligned} \tag{3}$$

where

$$A_x^k(z) = z + a_x^k g(z) + c_x^k h(z) \quad A_y^k(z) = a_y^k g(z) + c_y^k h(z)$$
$$B_x^k(z) = b_x^k g(z) + d_x^k h(z) \quad B_y^k(z) = z + b_y^k g(z) + d_y^k h(z)$$
$$C_x^k(z) = a_x^k g(z) + c_x^k h(z) \quad C_y^k(z) = a_y^k g(z) + c_y^k h(z)$$
$$D_x^k(z) = b_x^k g(z) + d_x^k h(z) \quad D_y^k(z) = b_y^k g(z) + d_y^k h(z). \tag{4}$$

Because the in-plane displacement fields are consisting of u_x, u_y, w, ϕ_x, ϕ_y, w_x and w_y, it is independent from the number of layers. The layerwise coefficients, a_x^k, a_y^k, b_x^k, b_y^k, c_x^k, c_y^k, d_x^k and d_y^k, are obtained from the constraint equations (more details are presented in Refs. [17, 18]) and are expressed in term of laminate geometry and material properties [17, 18].

2.2 Finite element implementation

To implement the layerwise theory into finite element model, the certain procedures should be introduced. The linear Lagrange interpolation function is employed to interpolate the in-plane displacements whereas the Hermite cubic interpolation function is used for the out-of-plane displacement interpolation [17, 18].

$$\left(u_x,\ u_y,\ \phi_x,\ \phi_y\right) = \sum_{m=1}^{n} N_m \left[\left(u_x\right)_m,\ \left(u_y\right)_m,\ \left(\phi_x\right)_m,\ \left(\phi_y\right)_m\right] \tag{5}$$

$$w = \sum_{m=1}^{n} \left[H_m\left(w\right)_m + H_{xm}\left(w_{,x}\right)_m + H_{ym}\left(w_{,y}\right)_m\right] \tag{6}$$

where N_m represents the Lagrange interpolation function and H_m, H_{xm} and H_{ym} represent the Hermite interpolation functions. The number of nodes in each element is n. The displacements in x and y-direction, rotations of the normal to the reference plane about x and y axes at m^{th} node in each element are denoted by $\left(u_x\right)_m$, $\left(u_y\right)_m$, $\left(\phi_x\right)_m$ and $\left(\phi_y\right)_m$, respectively. The displacement in z-direction and the partial derivatives for x and y directions at the m^{th} node in each element are w, $\left(w_{,x}\right)_m$ and $\left(w_{,y}\right)_m$, respectively.

$$\boldsymbol{u}_e = \boldsymbol{N}\boldsymbol{U} \tag{7}$$

$$\boldsymbol{u}_e = \left[u_x,\ u_y,\ w,\ \phi_x,\ \phi_y\right]^{\mathrm{T}} \tag{8}$$

$$\boldsymbol{N} = \begin{bmatrix} & N_m & 0 & 0 & 0 & 0 & 0 & 0 & \\ & 0 & N_m & 0 & 0 & 0 & 0 & 0 & \\ \cdots & 0 & 0 & H_m & H_{xm} & H_{ym} & 0 & 0 & \cdots \\ & 0 & 0 & 0 & 0 & 0 & N_m & 0 & \\ & 0 & 0 & 0 & 0 & 0 & 0 & N_m & \end{bmatrix} \tag{9}$$

where $\boldsymbol{U}$, $\boldsymbol{u}_e$ and $\boldsymbol{N}$ are global displacement, displacement of e-th element and shape function, respectively. Then the finite element procedure for static problem can be formulated as follows:

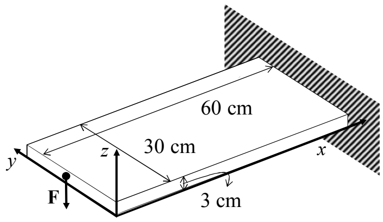

(a)

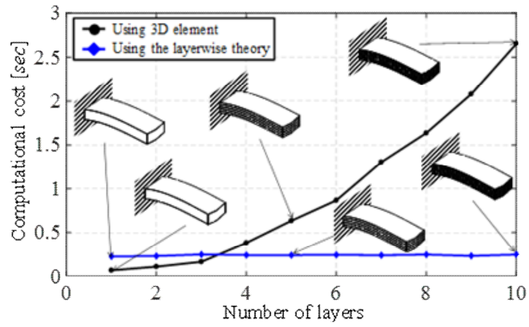

(b)

Fig. 2. A comparison of the computational times of 3D finite element procedure and the layerwise theory: E_1 = 139 GPa, $E_2 = E_3$ = 9.4 GPa, $G_{12} = G_{13}$ = 4.5 GPa, G_{23} = 2.89 GPa, $\nu_{12} = \nu_{13}$ = 0.02, ν_{23} = 0.33: (a) The analysis problem; (b) the computational time comparison.

$$\boldsymbol{K}\boldsymbol{U} = \boldsymbol{F} \tag{10}$$

$$\boldsymbol{k}_e = \iiint_V \boldsymbol{B}^{\mathrm{T}} \boldsymbol{Q}_e \boldsymbol{B}\, dV \tag{11}$$

$$\boldsymbol{B} = \boldsymbol{L}\boldsymbol{N} \tag{12}$$

where the global stiffness, the global force, the e-th elementary stiffness matrix and the constitutive matrix are denoted by $\boldsymbol{K}$ and $\boldsymbol{F}$, $\boldsymbol{k}_e$ and $\boldsymbol{Q}_e$, respectively. In order to reflect the influence due to the angle, the constitutive matrix is defined as follows:

$$\boldsymbol{Q}_e = \gamma_e^p \bar{\boldsymbol{Q}}_0. \tag{13}$$

The design variable and the penalty value are denoted by γ_e and p, respectively. To consider a rotational angle (θ) of ply, the transformation matrices, $\mathbf{T}_1$ and $\mathbf{T}_2$, are multiplied.

$$\bar{\boldsymbol{Q}}_0 = \boldsymbol{T}_1^{-1} \boldsymbol{Q}_0 \boldsymbol{T}_2. \tag{14}$$

The term $\boldsymbol{Q}_0$ represents the 3-dimensional constitutive matrix for orthotropic material.

As discussed in the previous chapter, the increase of the number of layers does not increase the computation time using the layerwise theory. To show this aspect numerically, a comparison between the computation times by general 3D elements and the present layerwise theory for the 3D solid structure in Fig. 2 are compared. The width, height and thickness of the analysis domain are 60 cm, 30 cm and 3 cm, respectively. The boundary condition and the applied force are shown in Fig. 2. Using the layerwise theory, the domain is discretized by 20x10x1. As a reference, the analysis domain is discretized with 8 node hexagonal finite element. The computational times solved by the finite elements formulated by the layer-wise theory and the 3D solid finite element procedure are compared by increasing the number of the layers from 1 to 10.

The number of degrees of freedom and the analysis time increase steadily by increasing the number of layers with the 3D finite element procedure. With the layerwise theory, the computation time is not significantly increased. Also, the maximum displacement obtained through 3d analysis is 4.4143, and the maximum displacement obtained through layerwise theory is 4.5446. The result obtained through layerwise theory is slightly larger, but there is no significant difference between two values.

2.3 Topology optimization formulation: Compliance minimization problem

The following formulation in Eq. (15) is the compliance minimization problem for laminate composite structure. Note that in the present formulation, the density parameters and the angles are optimized simultaneously.

$$\begin{aligned} &\underset{\gamma,\boldsymbol{\theta}}{\text{Minimize}} \quad C(\tilde{\gamma},\boldsymbol{\theta}) = \boldsymbol{F}^{\mathrm{T}}\boldsymbol{U} \\ &\text{Subject to} \quad V(\tilde{\gamma}) \le V^{*}. \end{aligned} \tag{15}$$

$\tilde{\gamma} = \Xi(\gamma)$ with the density filter Ξ

where compliance, global force, global displacement, the total volume and the maximum allowable volume are denoted by C, $\boldsymbol{F}$, $\boldsymbol{U}$, V and V^*, respectively. The design variables are denoted by γ and $\boldsymbol{\theta}$, and each vector indicates the topological density and angle of each layer. Also, Ξ means the density filtering. The sensitivity analyses for topological density and angles of layers are performed as follows:

$$\frac{dC}{d\tilde{\gamma}_e} = \frac{d\boldsymbol{F}^{\mathrm{T}}}{d\tilde{\gamma}_e}\boldsymbol{U} + \boldsymbol{F}^{\mathrm{T}}\frac{d\boldsymbol{U}}{d\tilde{\gamma}_e} = \boldsymbol{F}^{\mathrm{T}}\frac{d\boldsymbol{U}}{d\tilde{\gamma}_e}, \quad \frac{d\boldsymbol{F}^{\mathrm{T}}}{d\tilde{\gamma}_e} = 0 \tag{16}$$

$$\boldsymbol{K}\boldsymbol{U} = \boldsymbol{F}, \quad \frac{d\boldsymbol{K}}{d\tilde{\gamma}_e}\boldsymbol{U} + \boldsymbol{K}\frac{d\boldsymbol{U}}{d\tilde{\gamma}_e} = 0 \tag{17}$$

$$\frac{d\boldsymbol{U}}{d\tilde{\gamma}_e} = -\boldsymbol{K}^{-1}\frac{d\boldsymbol{K}}{d\tilde{\gamma}_e}\boldsymbol{U} \tag{18}$$

$$\frac{dC}{d\tilde{\gamma}_e} = -\boldsymbol{F}^{\mathrm{T}}\boldsymbol{K}^{-1}\frac{d\boldsymbol{K}}{d\tilde{\gamma}_e}\boldsymbol{U} \tag{19}$$

$$\frac{dC}{d\theta_k} = \frac{d\boldsymbol{F}^{\mathrm{T}}}{d\theta_k}\boldsymbol{U} + \boldsymbol{F}^{\mathrm{T}}\frac{d\boldsymbol{U}}{d\theta_k} = \boldsymbol{F}^{\mathrm{T}}\frac{d\boldsymbol{U}}{d\theta_k}, \quad \frac{d\boldsymbol{F}^{\mathrm{T}}}{d\theta_k} = 0 \tag{20}$$

$$\boldsymbol{K}\boldsymbol{U} = \boldsymbol{F}, \quad \frac{d\boldsymbol{K}}{d\theta_k}\boldsymbol{U} + \boldsymbol{K}\frac{d\boldsymbol{U}}{d\theta_k} = 0 \tag{21}$$

$$\frac{d\boldsymbol{U}}{d\theta_k} = -\boldsymbol{K}^{-1}\frac{d\boldsymbol{K}}{d\theta_k}\boldsymbol{U} \tag{22}$$

$$\frac{dC}{d\theta_k} = -\boldsymbol{F}^{\mathrm{T}}\boldsymbol{K}^{-1}\frac{d\boldsymbol{K}}{d\theta_k}\boldsymbol{U}. \tag{23}$$

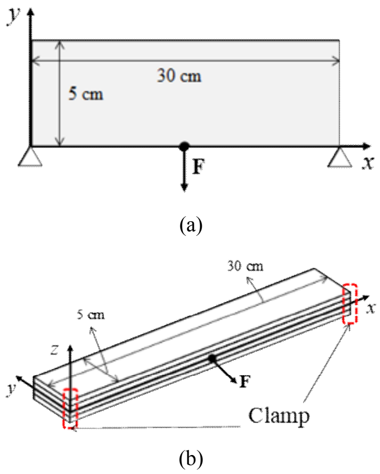

Fig. 3. MBB beam problem (The total number of elements in the design domain: 3750, **F**: -8000 N, thickness of each layer: 0.218 cm): (a) 2-dimensional view; (b) 3-dimensional view (E_1 = 132 GPa, $E_2 = E_3$ = 10.8 GPa, $G_{12} = G_{13}$ = 5.65 Gpa, G_{23} = 3.38 GPa, $\nu_{12} = \nu_{13}$ = 0.24, ν_{23} = 0.59).

The subscripts e and k, are the element number and the layer number, respectively. And $\boldsymbol{K}$ means global stiffness matrix.

3. Numerical examples

To show the validity of the developed topology optimization method, some numerical examples are considered in this chapter. For an optimization algorithm, the method of moving asymptotes is used [40].

3.1 Example 1: MBB beam

For the first example, the MBB beam structure with a composite layer is considered in Fig. 3. The two bottom points of the design domain are clamped and a downward static load with 8000 N is applied at the bottom center in Fig. 3. Unlike the topology optimization with a homogeneous material, the design domain is modeled with the composite layers with four layers in Fig. 3(b).

It is assumed that all the layers consist of T300/5208 carbon epoxy composite material in Fig. 3. In the present optimization, the angles of the plies are fixed to 0°, 0°, 0° and 0° degrees; the angles are excluded from the design variables. Fig. 4 solves the compliance minimization problem with the fixed angles in the optimization formulation Eq. (15) with 40 % mass constraint. Simply the result in Fig. 4 is optimized with the orthotropic material. Because the material is oriented parallel to the axes, the symmetric design can be obtained.

Fig. 5 solves the two optimization problems with the rotated angles (dash lines: The direction of the orientations of the fibers). As shown, the directionality of the plies causes the different designs. When the fibers align in x or y-direction, the symmetric optimal layout can be obtained in Fig. 4(a). How-

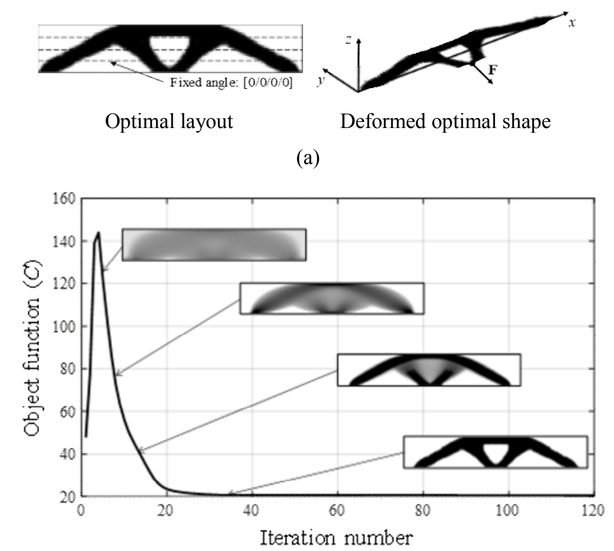

Fig. 4. Optimization result (compliance: 20.6208 J): (a) An optimal layout and deformed shape (scale factor: 5); (b) the object value history.

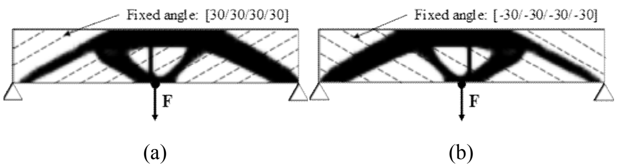

Fig. 5. Optimal layouts with the different angles (dash line: direction of the orientation of the fibers): (a) Angle: [30/30/30/30], compliance: 28.8847 J; (b) angle: [-30/-30/-30/-30], compliance: 28.8845 J.

ever, when the stiffness values have the directionality due to the rotations of the layers, i.e., 30 degrees or -30 degrees, the asymmetric optimal layouts can be obtained in Figs. 5(a) and (b). Due to the different rigidities in the parallel direction and the orthogonal direction of the plies, the thinner and the thicker arms do appear.

In the previous examples, it is observed that the different rigidities of the plies make some differences in the optimal layouts. As formulated in Eq. (15), it is also possible to optimize the angles of the plies simultaneously. Fig. 6 shows the optimal layout optimizing the angles of the plies with the same condition of the previous example. As shown in Fig. 6(b), the angles are optimized to increase the stiffness. The second and third layers are rotated counterclockwise by about 48 degrees. To prevent twist of composite material, their layers are laminated as symmetrically. So, this result can avoid structural issue like warping of composite. Also, the shape of right part becomes thicker with asymmetrical layout.

3.2 Example 2: MBB beam with an inclined force

Fig. 7 shows the optimal layout with the same conditions of the example 1 except the force condition. The inclined force

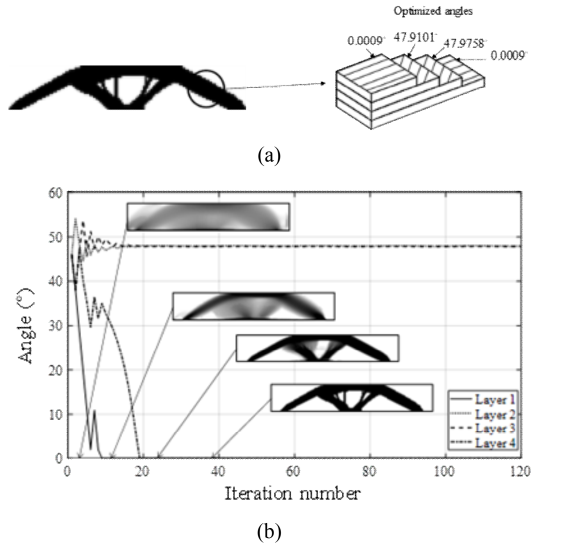

Fig. 6. Optimal layout and history of angle: (a) Optimal design (compliance: 17.9086 J); (b) the optimized history of the angles.

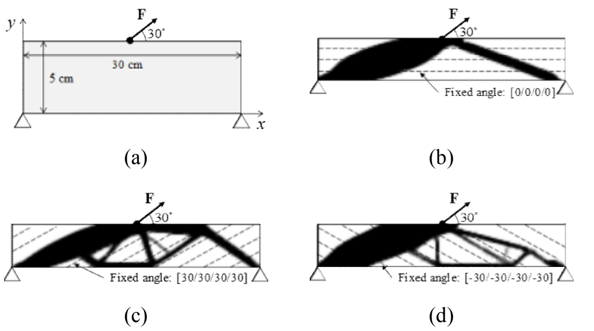

Fig. 7. Optimal results with constant ply angles (dash line: the direction of the fibers): (a) Design modain; (b) angle: [0/0/0/0], compliance: 5.1852 J and converged volume: 39.95 %; (c) angle: [30/30/30/30], compliance: 4.7712 J and converged volume: 39.79 %; (d) angle: [-30/-30/-30/-30], compliance: 12.4208 J and converged volume: 39.88 %.

applied at the top surface and the angles of the plies are set to constants. Because the load is applied in the direction of 30 degrees to the x-axis, the structural member in this direction becomes thicker than the other area.

With the inclinable force, all asymmetrical results are obtained. In addition, it is confirmed that the members in the direction in which the load is applied are thicker than the other parts in all the results. In Fig. 7(c), the thickness of the opposite direction of the load is the smallest. This is because the orientation of each layer is set to -30 degrees, and the stiffness in this direction is higher than the other results. As observed in the previous example, the angles of the plies are optimized with the inclined force and result is presented in Fig. 8. And the lowest compliance is drawn with optimization of angle of plies.

3.3 Example 3: Square frame

Fig. 9 considers a squared design domain with in-plane and

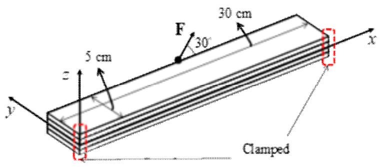

(a)

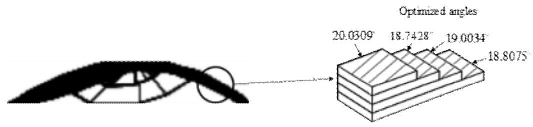

(b)

Fig. 8. Design domain and an optimal layout: (a) Design domain; (b) an optimal layout and the angle of each layer (Compliance: 3.4193 J).

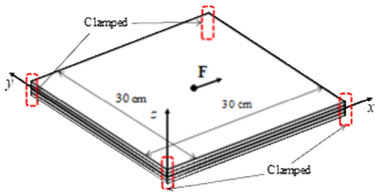

(a)

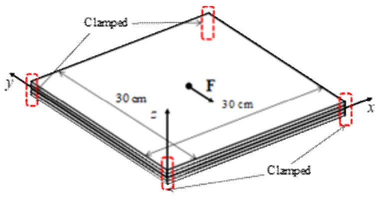

(b)

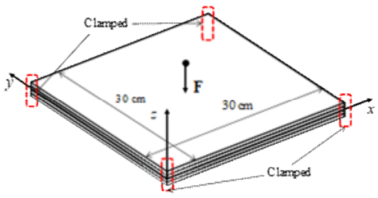

(c)

Fig. 9. Square design domain (Total number of elements in the design domain: 4900, thickness of each layer: 0.218 cm, E_1 = 132 GPa, $E_2 = E_3$ = 10.8 GPa, $G_{12} = G_{13}$ = 5.65 Gpa, G_{23} = 3.38 GPa, $v_{12} = v_{13}$ = 0.24, v_{23} = 0.59): (a) x-direction load: 8000 N; (b) y-direction load: 8000 N; (c) z-direction load: 8000 N.

out-of-plane loads with the fixed four corners. Magnitude of loads are 8000N for all cases and direction is presented in Fig. 9. All optimal shapes are presented in Fig. 10.

Basically, last one has different shape (horizontal shape structure) from first and second results (x-shaped structures) in Fig. 10(a) because in the first two results, the in-plane loads are considered, and the final result is that the out-of-plane load is taken into account. Also, Fig. 10 shows the optimal results with 0 and 20 degrees for all load cases. The differences in the stiffness in each direction cause the differences in the designs. With the force in the z-direction, the structures aligned in the fiber's direction, i.e., 0 or 20 degrees, can be obtained.

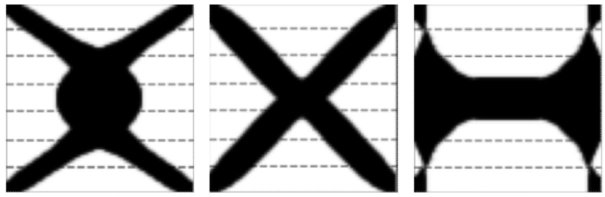

x-direction load	y-direction load	z-direction load
3.8731 J	5.6473 J	1.3993x10^4 J

(a)

x-direction load	y-direction load	z-direction load
3.4557 J	5.0568 J	1.0843x10^4 J

(b)

Fig. 10. Optimal results with the fixed angles of the plies (dash line: the direction of the fibers): (a) Fixed angle: [0/0/0/0]; (b) fixed angle: [20/20/20/20].

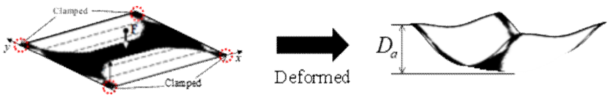

(a)

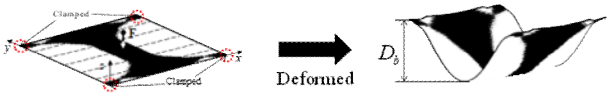

(b)

Fig. 11. Difference in deformation according to direction of the material distribution: (a) Strong stiffness direction (D_a = 1.7491 cm); (b) weak stiffness direction (D_a = 2.8108 cm).

To check the validity of the above optimized results, Fig. 11 compared the deformations of the optimized layouts with the rotated plies. With the optimized layout of Fig. 11(a), the deformation is successfully decreased when the large deformation is observed with the rotated plies of Fig. 11(b).

Then we can simultaneously optimize the layouts and the angles of the plies in Fig. 12. As illustrated, the inclusion of the angles of the plies causes some differences in the optimized layouts. With the square shaped design domain, Figs. 12(a) and (b) are the 90 degrees rotated designs to each other. With the z-direction force in Fig. 12(c), the different design is obtained. Unlike the previous two designs, the bending type design is obtained.

3.4 The effect of angles and the comparison of the computational costs

The overall stiffness of composite layer being highly dependent on the angle of the plies, we more teste the effect of

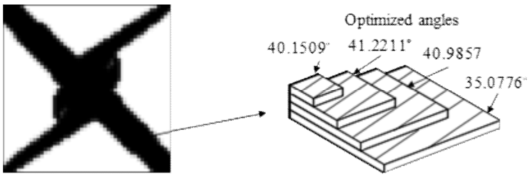

(a) x-direction load, compliance: 3.5791 J

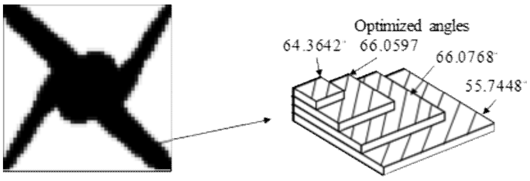

(b) y-direction load, compliance: 3.5237 J

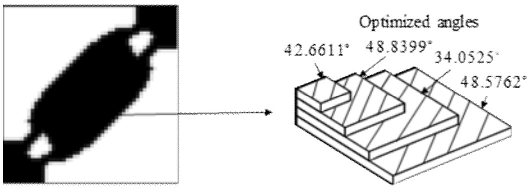

(c) z-direction load, compliance: 2.9625x10^3 J

Fig. 12. Optimal result with each load case: (a) Optimal layout for x-direction load (Compliance: 3.5791 J); (b) optimal layout for x-direction load (Compliance: 3.5237 J), (c) optimal layout for x-direction load (Compliance: 2.9625x10^3 J).

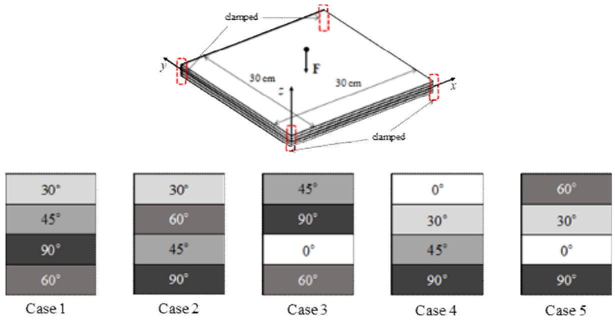

Fig. 13. Different angle configurations for the 3rd load condition of Fig. 9.

angles in Fig. 13.

To investigate the effect of the stacked angles, the five angles, 0°, 30°, 45°, 60° and 90°, were selected and the five combinations of Fig. 13 are tested in Fig. 14. As shown, the optimized layouts are influenced very much.

4. Conclusions

The present study develops a new topology optimization technique for a laminated composite structure with the layerwise theory. Although some relevant researches performed the topology optimization with classical plate theory, it is not rare to consider the topology optimization with the layerwise theory. Laminate structures with large thickness of each layer are not expected to be highly accurate when analyzed using classical plate theory. One of the methods developed to solve this problem is the layerwise theory. In composite structures with

(a) (b) (c)

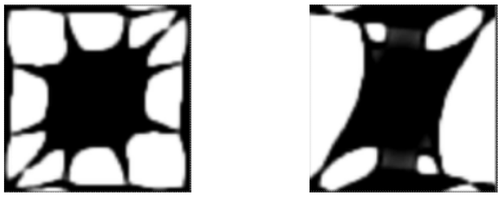

(d) (e)

Fig. 14. Optimized layouts with the different combinations of Fig. 13: (a) Case 1 (compliance: 7782.85 J); (b) case 2 (compliance: 8261.16 J); (c) case 3 (compliance: 6887.84 J); (d) case 4 (compliance: 6221.22 J); (e) case 5 (compliance: 9571.85 J).

some layers, the improved theories like the layerwise theory are required to improve the accuracy of in-plane displacements and stress. Furthermore, the computation time can be significantly saved with the layerwise theory. From the results of this research, it is drawn that the optimized shape varies with angle of layers. Even with the same optimization problem, different optimal shapes are obtained when the rotation angles of all layers are different. Also, it is important to optimize the angles of plies to minimize the compliance. In addition, the present study shows that the optimal layouts and the optimal angles of plies are depending on the direction of the loads. Several examples show that there is a difference in the direction of material distribution when in-plane load is applied, and out-of-plane load is applied.

Acknowledgments

This work was supported by the National Research Foundation of Korea (NRF) grant funded by the Korea government (MSIT)(No.2018R1A5A7025522) and was supported by the National Research Foundation of Korea (NRF) Grant [No: 2014M3A6B3063711(Global Frontier R&D Program on Center for Wave Energy Control based on Metamaterials)] funded by the Korean Ministry of Science, ICT and Future Planning (MSIP).

References

[1] J. N. Reddy, *Mechanics of Laminated Composite Plates and Shells, Theory and Analysis*, CRC Press (2004).

[2] N. P. Suh, *Axiomatic Design and Fabrication of Composite Structures: Applications in Robots, Machine Tools, and Automobiles*, Oxford University Press (2005).

[3] X. Zhou, A. Chattopadhyay and H. S. Kim, An efficient layerwise shear-deformation theory and finite element implementation, *Journal of Reinforced Plastics and Compos-*

ites, 23 (2004) 131-152.

[4] R. Mindlin, Influence of rotary inertia and shear on flexural motions of isotropic elastic plates, *Journal of Applied Mechanics-Transactions of the ASME* (1951).

[5] J. Whitney and N. Pagano, Shear deformation in heterogeneous anisotropic plates, *Journal of Applied Mechanics*, 37 (1970) 1031-1036.

[6] J. N. Reddy, A simple higher-order theory for laminated composite plates, *Journal of Applied Mechanics*, 51 (1984) 745-752.

[7] A. Chattopadhyay and H. Gu, New higher order plate theory in modeling delamination buckling of composite laminates, *AIAA Journal*, 32 (1994) 1709-1716.

[8] E. Barbero, J. Reddy and J. Teply, General two-dimensional theory of laminated cylindrical shells, *AIAA Journal*, 28 (1990) 544-553.

[9] J. Reddy, A generalization of two-dimensional theories of laminated composite plates, *International Journal for Numerical Methods in Biomedical Engineering*, 3 (1987) 173-180.

[10] A. Toledano and H. Murakami, A composite plate theory for arbitrary laminate configurations, *Journal of Applied Mechanics*, 54 (1987) 181-189.

[11] K. M. Rao and H.-R. Meyer-Piening, Analysis of thick laminated anisotropic composite plates by the finite element method, *Composite Structures*, 15 (1990) 185-213.

[12] E. Carrera, Evaluation of layerwise mixed theories for laminated plates analysis, *AIAA Journal*, 36 (1998) 830-839.

[13] D. Sciuva, An improved shear-deformation theory for moderately thick multilayered anisotropic shells and plates, *Journal of Applied Mechanics*, 54 (1987) 589-596.

[14] K. Bhaskar and T. Varadan, A higher-order theory for bending analysis of laminated shells of revolution, *Computers & Structures*, 40 (1991) 815-819.

[15] P. B. Xavier, K. Lee and C. Chew, An improved zig-zag model for the bending of laminated composite shells, *Composite Structures*, 26 (1993) 123-138.

[16] H. S. Kim, X. Zhou and A. Chattopadhyay, Interlaminar stress analysis of shell structures with piezoelectric patch including thermal loading, *AIAA Journal*, 40 (2002) 2517-2525.

[17] H. S. Kim, A. Chattopadhyay and A. Ghoshal, Characterization of delamination effect on composite laminates using a new generalized layerwise approach, *Computers & Structures*, 81 (2003) 1555-1566.

[18] H. S. Kim, A. Chattopadhyay and A. Ghoshal, Dynamic analysis of composite laminates with multiple delamination using improved layerwise theory, *AIAA Journal*, 41 (2003) 1771-1779.

[19] O. Sigmund, A 99 line topology optimization code written in Matlab, *Structural and Multidisciplinary Optimization*, 21 (2001) 120-127.

[20] K. Suzuki and N. Kikuchi, A homogenization method for shape and topology optimization, *Computer Methods in Applied Mechanics and Engineering*, 93 (1991) 291-318.

[21] M. P. Bendsoe and O. Sigmund, *Topology Optimization: Theory, Methods, and Applications*, Springer Science & Business Media (2013).

[22] M. P. Bendsøe and N. Kikuchi, Generating optimal topologies in structural design using a homogenization method, *Computer Methods in Applied Mechanics and Engineering*, 71 (1988) 197-224.

[23] G. H. Yoon, J. S. Jensen and O. Sigmund, Topology optimization of acoustic–structure interaction problems using a mixed finite element formulation, *International Journal for Numerical Methods in Engineering*, 70 (2007) 1049-1075.

[24] G. H. Yoon, Topology optimization for turbulent flow with Spalart–Allmaras model, *Computer Methods in Applied Mechanics and Engineering*, 303 (2016) 288-311.

[25] G. H. Yoon, J. H. Kim, K. O. Jung and J. W. Jung, Transient quasi-static Ritz vector (TQSRV) method by Krylov subspaces and eigenvectors for efficient contact dynamic finite element simulation, *Applied Mathematical Modelling*, 39 (2015) 2740-2762.

[26] G. H. Yoon, Stress-based topology optimization method for steady-state fluid–structure interaction problems, *Computer Methods in Applied Mechanics and Engineering*, 278 (2014) 499-523.

[27] J. W. Lee, G. H. Yoon and S. H. Jeong, Topology optimization considering fatigue life in the frequency domain, *Computers & Mathematics with Applications*, 70 (2015) 1852-1877.

[28] G. H. Yoon, Maximizing the fundamental eigenfrequency of geometrically nonlinear structures by topology optimization based on element connectivity parameterization, *Computers & Structures*, 88 (2010) 120-133.

[29] W. Hansel and W. Becker, Layerwise adaptive topology optimization of laminate structures, *Engineering Computations*, 16 (1999) 841-851.

[30] W. Hansel, A. Treptow, W. Becker and B. Freisleben, A heuristic and a genetic topology optimization algorithm for weight-minimal laminate structures, *Composite Structures*, 58 (2002) 287-294.

[31] M. Bruggi, G. Milani and A. Taliercio, Design of the optimal fiber-reinforcement for masonry structures via topology optimization, *International Journal of Solids and Structures*, 50 (2013) 2087-2106.

[32] S. N. Sørensen and E. Lund, Topology and thickness optimization of laminated composites including manufacturing constraints, *Structural and Multidisciplinary Optimization*, 48 (2013) 249-265.

[33] G. P. Rodrigues, J. Guedes and J. Folgado, Combined topology and stacking sequence optimization of composite laminated structures for structural performance measures, *4th Engineering Optimization Conference* (2015).

[34] S. R. Henrichsen, *Optimization of Laminated Composite Structures,* Aalborg Universitet (2015).

[35] P. Coelho, J. Guedes and H. Rodrigues, Multiscale topology optimization of bi-material laminated composite structures, *Composite Structures*, 132 (2015) 495-505.

[36] C. J. Rupp, A. Evgrafov, K. Maute and M. L. Dunn, Design

of piezoelectric energy harvesting systems: A topology optimization approach based on multilayer plates and shells, *Journal of Intelligent Material Systems and Structures*, 20 (2009) 1923-1939.

[37] B. Zheng, C.-J. Chang and H. C. Gea, Topology optimization of energy harvesting devices using piezoelectric materials, *Structural and Multidisciplinary Optimization*, 38 (2009) 17-23.

[38] C. Y. Kiyono, E. C. N. Silva and J. Reddy, Design of laminated piezocomposite shell transducers with arbitrary fiber orientation using topology optimization approach, *International Journal for Numerical Methods in Engineering*, 90 (2012) 1452-1484.

[39] C. Kiyono, E. Silva and J. Reddy, Optimal design of laminated piezocomposite energy harvesting devices considering stress constraints, *International Journal for Numerical Methods in Engineering*, 105 (2016) 883-914.

[40] K. Svanberg, The method of moving asymptotes—a new method for structural optimization, *International Journal for Numerical Methods in Engineering*, 24 (1987) 359-373.

Appendix

$$\boldsymbol{L}=\left[\begin{array}{ccccccc} & \frac{\partial}{\partial x} & 0 & C_1^k\frac{\partial^2}{\partial x^2}+D_1^k\frac{\partial^2}{\partial x\partial y} & A_1^k\frac{\partial}{\partial x} & B_1^k\frac{\partial}{\partial x} & \\ & 0 & \frac{\partial}{\partial y} & C_2^k\frac{\partial^2}{\partial x\partial y}+D_2^k\frac{\partial^2}{\partial y^2} & A_2^k\frac{\partial}{\partial y} & B_2^k\frac{\partial}{\partial y} & \\ & 0 & 0 & 0 & 0 & 0 & \\ \cdots & 0 & 0 & C_{2,z}^k\frac{\partial}{\partial x}+\left(1+D_{2,z}^k\right)\frac{\partial}{\partial y} & A_{2,z}^k & B_{2,z}^k & \cdots \\ & 0 & 0 & \left(C_{1,z}^k+1\right)\frac{\partial}{\partial x}+D_{1,z}^k\frac{\partial}{\partial y} & A_{1,z}^k & B_{1,z}^k & \\ & \frac{\partial}{\partial y} & \frac{\partial}{\partial x} & C_2^k\frac{\partial^2}{\partial x^2}+\left(C_1^k+D_2^k\right)\frac{\partial^2}{\partial x\partial y}+D_1^k\frac{\partial^2}{\partial y^2} & A_1^k\frac{\partial}{\partial y}+A_2^k\frac{\partial}{\partial x} & B_1^k\frac{\partial}{\partial y}+B_2^k\frac{\partial}{\partial x} & \end{array}\right] \tag{A.1}$$

$$\boldsymbol{T}_1=\begin{bmatrix} \cos^2\theta & \sin^2\theta & 0 & 0 & 0 & 2\cos\theta\sin\theta \\ \sin^2\theta & \cos^2\theta & 0 & 0 & 0 & -2\cos\theta\sin\theta \\ 0 & 0 & 1 & 0 & 0 & 0 \\ 0 & 0 & 0 & \cos\theta & -\sin\theta & 0 \\ 0 & 0 & 0 & \sin\theta & \cos\theta & 0 \\ -\cos\theta\sin\theta & \cos\theta\sin\theta & 0 & 0 & 0 & \cos^2\theta-\sin^2\theta \end{bmatrix} \tag{A.2}$$

$$\boldsymbol{T}_2=\begin{bmatrix} \cos^2\theta & \sin^2\theta & 0 & 0 & 0 & \cos\theta\sin\theta \\ \sin^2\theta & \cos^2\theta & 0 & 0 & 0 & -\cos\theta\sin\theta \\ 0 & 0 & 1 & 0 & 0 & 0 \\ 0 & 0 & 0 & \cos\theta & -\sin\theta & 0 \\ 0 & 0 & 0 & \sin\theta & \cos\theta & 0 \\ -2\cos\theta\sin\theta & 2\cos\theta\sin\theta & 0 & 0 & 0 & \cos^2\theta-\sin^2\theta \end{bmatrix} \tag{A.3}$$

$$\boldsymbol{Q}_0=\Gamma\cdot\begin{bmatrix} E_1\left(1-\nu_{23}\nu_{32}\right) & E_1\left(\nu_{21}+\nu_{31}\nu_{23}\right) & E_1\left(\nu_{31}+\nu_{21}\nu_{32}\right) & 0 & 0 & 0 \\ E_1\left(\nu_{21}+\nu_{31}\nu_{23}\right) & E_2\left(1-\nu_{13}\nu_{31}\right) & E_2\left(\nu_{32}+\nu_{12}\nu_{31}\right) & 0 & 0 & 0 \\ E_1\left(\nu_{31}+\nu_{21}\nu_{32}\right) & E_2\left(\nu_{32}+\nu_{12}\nu_{31}\right) & E_3\left(1-\nu_{12}\nu_{21}\right) & 0 & 0 & 0 \\ 0 & 0 & 0 & G_{23} & 0 & 0 \\ 0 & 0 & 0 & 0 & G_{13} & 0 \\ 0 & 0 & 0 & 0 & 0 & G_{12} \end{bmatrix} \tag{A.4}$$

$$\Gamma=\frac{1}{1-\nu_{12}\nu_{21}-\nu_{23}\nu_{32}-\nu_{31}\nu_{13}-2\nu_{21}\nu_{32}\nu_{13}} \tag{A.5}$$

where E_i, G_{ij} and ν_{ij} mean the Young's modulus in the *i*-direction, the shear modulus in the *ij*-plane and Poisson's ratio between *i* and *j*-direction.

Jong Wook Lee received his B.S. degree in Mechanical Engineering from Kyungpook National University, Daegu, Korea in 2010. He got his Ph.D. degree in the Department of Mechanical Engineering, Hanyang University. His research interests include topology optimization, static failure and dynamic failure, composite material.

Jong Jin Kim received his B.S. degree in Mechanical Engineering from Gangneung Wonju National University, Gangwon, Korea in 2017. He is currently a student at School of Mechanical Engineering, Hanyang University, Seoul, Republic of Korea. His research interests are topology optimization and composite material.

Heung Soo Kim received his B.S. and M.S. degrees in the Department of Aerospace Engineering from Inha University, Korea in 1997 and 1999, respectively. He got his Ph.D. degree in the Department of Mechanical and Aerospace Engineering from Arizona State University in 2003. He is now working a Professor in the Department of Mechanical, Robotics and Energy Engineering, Dongguk University. His main research interests are in biomimetic actuators and sensors, smart materials and structures as applied to aerospace structures and vehicles.

Gil Ho Yoon received his B.S. degree in Mechanical and Aerospace Engineering from Seoul National University in 1998. And he received his M.S. and Ph.D. degrees in Mechanical and Aerospace Engineering from Seoul National University in 2000 and 2004, respectively. Dr. Yoon is currently a Professor at School of Mechanical Engineering, Hanyang University, Seoul, Republic of Korea.